Journal of Orthodontic and Periodontal Biomaterials Research

2023, Volume 3, Issue 2, Page No: 33-47

Available online at: https://galaxypub.co/

Galaxy Publication

Influence of Defect Configuration on Alveolar Ridge Preservation Outcomes: An In Vivo Experimental Study

Miguel Vega[1], Miguel Sanchez[2], Sofia N. Garcia[2], Sofia I. Garcia[1]*, Camila W. Gonzalez[1]

[1]Department of Orthodontics and Dentofacial Orthopedics, School of Dentistry, National University of Colombia, Bogotá, Peru.
[2]Department of Periodontology and Oral Implantology, School of Dentistry, University of Buenos Aires, Buenos Aires, Peru.

***E-mail** ✉ sofia.garcia.enamel@hotmail.com

Received: 17 May 2023; **Revised:** 22 August 2023; **Accepted:** 24 August 2023

ABSTRACT

The purpose of this study was to compare the bone healing potential of 1-, 2-, and 3-wall defects following alveolar ridge preservation (ARP) treatment, as well as to evaluate the efficacy of ARP as a treatment option for destructive sites. Three groups, characterized by 1-, 2-, and 3-wall defects, were randomly assigned to the maxillary second, third, and fourth premolars in each of 8 beagle dogs. Each defect was created at either the mesial or distal root site of the tooth, which was hemi-sectioned and extracted. The contralateral root was preserved to superimpose with the experimental site for histomorphometric analysis. For each site, either spontaneous healing (SH; control) or ARP (test intervention) was randomly applied. Each group was divided in half and underwent a healing period of either 4 or 12 weeks. The Mann-Whitney *U* test and Kruskal-Wallis test were used for histomorphometric analyses. Statistical significance was set at $P<0.05$. Qualitative analysis revealed a higher percentage of new bone in the apical area compared to the coronal area, regardless of defect type and healing period. In quantitative analysis, the 3-wall defect exhibited a significantly higher percentage of mineralization in the ARP group afier 12 weeks of healing (ARP: 61.73%±7.52%; SH: 48.84%±3.06%; $P=0.029$).An increased percentage of mineralization was observed with a greater number of remaining bony walls, although this finding did not reach statistical significance. Within the limitations of this study, ARP treatment for compromised sockets appears to yield a higher percentage of mineralization compared to SH. Although the effectiveness of the remaining bony walls was limited, their presence appeared to improve the percentage of mineralization in ARP treatment.

Keywords: Alveolar ridge augmentation, Bone regeneration, Bone substitutes, Histology, Tooth extraction

How to Cite This Article: Vega M, Sanchez M, Garcia SN, Garcia SI, Gonzalez CW. Influence of Defect Configuration on Alveolar Ridge Preservation Outcomes: An In Vivo Experimental Study. J Orthod Periodontal Biomater Res. 2023;3(2):33-47. https://doi.org/10.51847/9nAerUHVD3

Introduction

In a systematic review, the resorption of socket walls after tooth extraction reportedly resulted in a reduction of 3.79 mm in the horizontal dimension of the alveolar ridge and 1.24 mm in the vertical dimension at 6 months, corresponding to a 29% to 63% decrease [1]. Such reductions in ridge dimensions can impede the optimal positioning of dental implants and the achievement of sufficient primary stability. To minimize alveolar ridge resorption after tooth extraction, the use of bone substitutes for alveolar ridge preservation (ARP) has been proposed [2, 3]. Although ARP does not completely prevent the loss of the alveolar ridge prior to tooth extraction, as the term might suggest, it is expected to maintain sufficient bone volume for subsequent implant placement [4-6].

In clinical scenarios, tooth extraction is performed in cases of periodontitis and/or endodontic-periodontal combined lesions. Periodontally compromised teeth can lead not only to alveolar ridge shrinkage but also to

unpredictable or delayed healing of the extraction socket [7-9]. To improve the feasibility of implant placement, various studies on extraction socket management using ARP at periodontally compromised sites have been conducted [10-12].

Recent clinical research on the application of ARP in periodontally compromised extraction sockets demonstrated a high safety rate of 99.3%. This rate encompasses sites that healed uneventfully and those with controllable infections following ARP. ARP in periodontally compromised sockets is believed to increase the feasibility of implant placement and to increase bone volume compared to sockets with no intervention after tooth extraction [13-15]. Although ARP can minimize changes in alveolar dimensions with a high safety rate, histological and radiographic outcomes have varied considerably [16, 17]. These variations may be attributed to the differing healing potentials of extraction sockets, which can be influenced by the condition of the bone walls [9].

In clinical settings, some periodontally compromised sites may display insufficient new bone formation and inadequate augmented bone volume even after ARP, necessitating additional bone augmentation at the time of implant placement [15]. Understanding the prognosis of ARP based on bone configuration is important for both clinicians and patients in terms of the cost and efficacy of ridge preservation procedures. This knowledge can improve comprehension and cooperation throughout the regenerative treatment process.

A positive correlation between the number of bone walls and healing potential has been demonstrated in various studies concerning regenerative procedures [18-21]. However, limited evidence is available regarding the quantitative analysis of bone configuration in extraction sockets and the outcomes of ARP. To establish an evidence-based approach to managing extraction sockets based on bone configuration, the relationship between the bone walls and the outcomes of ARP must be explored. In a 3-wall defect ARP model using beagle dogs, the ingrowth of new bone into biomaterials from pristine bone was observed at 4 weeks through histologic and radiographic examination [22]. Additionally, collagen membranes have been shown to be resorbed within 12 weeks [23].

The purpose of this study was to compare the bone healing potential in 1-, 2-, and 3-wall defects following ARP over 4- and 12-week healing periods using histologic analyses.

Materials and Methods

Ethics statement

The experiment adhered to the principles of the 3 Rs (Replacement, Reduction, and Refinement), and the experimental protocol received approval from the Institutional Animal Care and Use Committee of Seoul National University (No. SNU-200619-1-1). The manuscript was prepared in accordance with the ARRIVE 2.0 guidelines [24].

Sample size calculation

The sample size was calculated using G*Power (version 3.1.9.7, University of Düsseldorf, Düsseldorf, Germany). Due to the absence of prior preclinical studies comparing the outcomes of ARP across 3 bone wall configurations, the sample size for this study was estimated based on the assumption that the amount of newly formed bone would increase with the number of bone walls present. The anticipated mean difference and standard deviation (SD) among the 3 groups were set at 9% and 3%, respectively. Based on a significance level (α) of 5% and a power (1 − β) of 80%, we determined that 4 samples per group would be required. To assess the development of new bone at 2 time points (4 and 12 weeks after tooth extraction), 8 samples were needed for each configuration. Since 3 bone wall configurations could be created at the maxillary second, third, and fourth premolars in a single animal, a total of 8 animals were utilized for this study.

Experimental animals

Eight male beagle dogs, approximately 1 year old and weighing between 10 and 12 kg, were utilized in this preclinical study. At the time of recruitment, all animals were in good systemic and periodontal health, and their dentition was normal. Before the experiment began, the animals underwent a 2-week acclimation period at the facility. Each dog was housed in an individual indoor kennel measuring 90 cm wide, 80 cm deep, and 80 cm high. They had free access to water and were fed a standard pellet dog food diet.

Study design

Three defect types, specifically 1-wall, 2-wall, and 3-wall defects, were randomly assigned to the maxillary second, third, and fourth premolars **(Figure 1a)**. The study utilized a split-mouth design, with spontaneous healing (SH) serving as the control and ARP as the test intervention. One site was located on the mesial root of the tooth on the left side, while the other was on the distal root of the tooth on the right side, enabling the superimposition of the retained contralateral tooth during histomorphometric analysis. Complete blinding during or after the procedure was not feasible due to the discernible presence of the bone substitute.

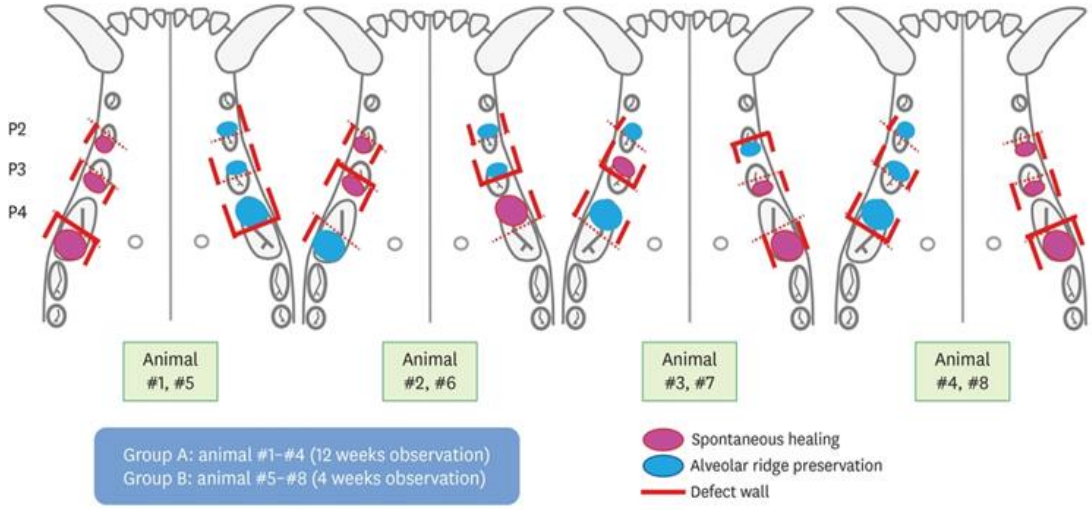

a

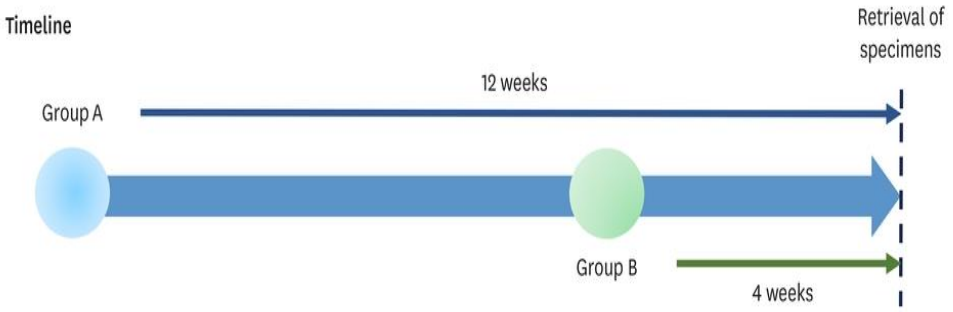

b

Figure 1. In the split-mouth design, one of the hemi-sectioned roots was randomly allocated to either 1) the spontaneous healing group or 2) the alveolar ridge preservation group. The contralateral roots served as a reference for the alveolar ridge.

Experimental biomaterials

The ARP group underwent ridge preservation after tooth extraction, utilizing collagenated deproteinized porcine bone mineral (THE Graft Collagen, Purgo, Seongnam, Korea). A crosslinked collagen membrane (The Cover, Purgo) was trimmed to approximately match the size of the defect and then placed over the site, followed by the application of collagenated deproteinized porcine bone mineral at the ARP site.

Experimental procedures

The timeline of this study is illustrated in **Figure 1b**. Four beagle dogs in each group underwent hemisection of the root and creation of a bony defect. Subsequently, each defect was subjected to either SH or ARP, with designated healing periods of 4 or 12 weeks for each group.

Presurgical anesthesia

For the surgical procedure, general anesthesia was induced with an intravenous injection of a 1:1 combination of tiletamine hydrochloride and zolazepam hydrochloride (0.1 mg/kg, Zoletil, Virbac, Carros, France), xylazine (2.3

mg/kg, Rompun, Bayer Korea, Ansan, Korea), and atropine sulfate (0.05 mg/kg, Jeil Pharm., Daegu, Korea). Subsequently, local anesthesia was administered by injecting 2% lidocaine HCl with 1:1,000,000 epinephrine (Huons, Seongnam, Korea).

Defect creation and ridge preservation

The surgical interventions are depicted in **Figure 2**. Intracrevicular incisions were made in the maxillary premolar region, followed by flap elevation. The maxillary second, third, and fourth premolars (PM2, PM3, and PM4) were hemisected using a diamond bur (TC-21, Kiyohara Industrial Park, Utsunomiya, Japan). Root canal treatment was performed on the pulp of the root intended to be retained, using a 25 mm K-file (#15 and #20, MANI, Inc., Utsunomiya, Japan) and a Ni-Ti file (Protaper Universal SX, F1, F2, and F3, Dentsply Maillefer, Ballaigues, Switzerland). Following root preparation, a calcium hydroxide-based root canal sealer (cleaniCal, Maruchi, Wonju, Korea) was applied. Subsequently, the root was sealed with a cotton pellet and an intermediate restorative material (Dentsply Sirona, Milford, DE, USA).

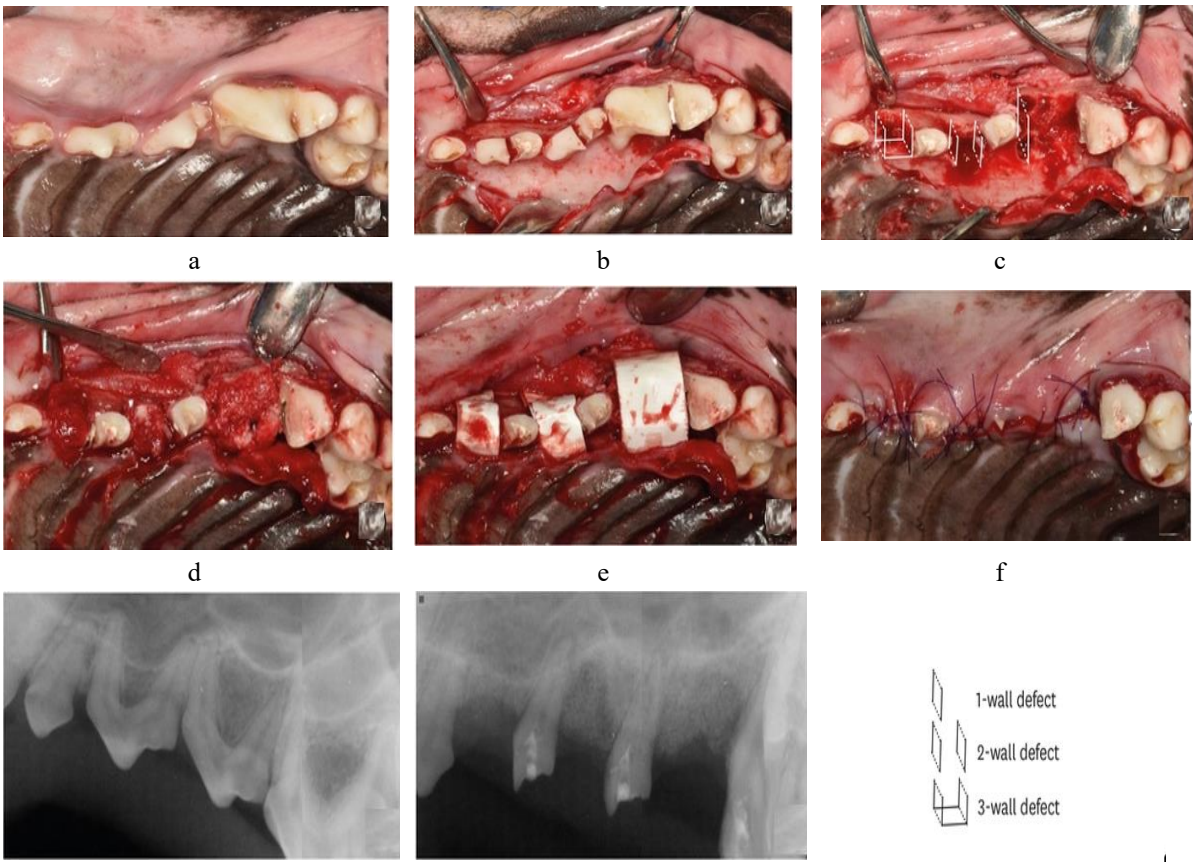

Figure 2. Clinical photographs and radiographs. (a) Preoperative clinical photographs. (b, c) Intraoperative clinical photographs. Following the extraction of each hemi-sectioned root, bony defects were created. (d-f) Alveolar ridge preservation was performed, or not, at each site in a randomized split-mouth design. (g, h) Periapical radiographs before and after surgery, respectively.

At the experimental site, the root was extracted, and a 1-, 2-, or 3-wall defect was created using a #4 round bur in accordance with the random assignment. The resulting defect size and morphology after tooth extraction were as follows:

- For the 1-wall defect, the buccal, lingual, and mesial (or distal) walls were removed, exposing the hemisected root surface.
- For the 2-wall defect, the buccal and lingual bone walls were removed.
- For the 3-wall defect, only the buccal bone wall was removed.

The height (10 mm) and mesiodistal width of the root at the experimental site were measured using a Williams probe. Root planing was performed on the remaining exposed roots to completely remove the periodontal ligament. Ridge preservation was then applied according to the random allocation, utilizing collagenated deproteinized porcine bone mineral and a double-layered crosslinked collagen membrane. Flap advancement was executed to achieve primary closure of the surgical site using 4/0 Vicryl sutures (Ethicon Inc, Raritan, NJ, USA). These surgical procedures and radiographs are illustrated in **Figure 2**.

Animal care and monitoring

The animals received an intravenous administration of antibiotics (20 mg/kg Cefazolin, Chongkundang Pharmaceutical Corp., Seoul, Korea), analgesics (5 mg/kg Toranzin, Samsung Pharm., Hwaseong, Korea), and antispasmodics (0.05 mg/kg atropine sulfate, Jeil Pharm.) following surgery. Additionally, antibiotics (500 mg amoxicillin, Chongkundang Pharmaceutical Corp.) and analgesics (400 mg ibuprofen, Daewoong Pharm., Seoul, Korea) were mixed into the animals' diet for 3 days after surgery. Sutures were removed 10 days after the procedure. Oral hygiene was maintained with a 0.12% chlorhexidine gluconate solution (Hexamedine, Bukwang Pharm., Seoul, Korea) biweekly.

Euthanasia of animals

The animals were euthanized at 4 and 12 weeks post-surgery by carotid injection with potassium chloride (75 mg/kg, Jeil Pharm.). Block biopsies including the experimental sites were harvested for histologic analyses.

Histological processing

Block sections, including experimental segments, were fixed in 10% neutral buffered formalin for 2 weeks. Following fixation, the sections were rinsed in sterile water and decalcified in 5% formic acid for 10 days. They were then dehydrated using a graded ethanol series and embedded in paraffin. A block of the tooth, encompassing the remaining root and surgical site, was harvested based on the mesiodistal length of the hemi-sectioned tooth. Subsequently, the most central sections of each remaining root and surgical site within each block were identified for analysis. Step-serial sections, 5 μm thick, were cut in the buccolingual vertical plane. Masson trichrome staining was applied to each selected slide to facilitate histological and histometric analyses.

Histological and histomorphometric analyses

Histological samples were scanned for digital transformation and analyzed using digital microscopy software (CaseViewer, 3DHISTECH, Budapest, Hungary).

Qualitative histometric analyses of defect sites involved defining a 1 mm × 1 mm rectangular region of interest (ROI) in the apical, middle, and coronal areas of the histological samples **(Figures 3 and 4)**. Assuming that the contralateral root of the same tooth would be symmetrical, we superimposed a reference image of the contralateral root onto the image of the defect site to locate the ROIs in the area under investigation. This was done with reference to the sinus floor and the contour of the residual alveolar bone. From the midpoint of the line across the buccopalatal alveolar crest to the center of the root apex, the apical, middle, and coronal ROIs were set based on vertical depth. These were magnified 9-fold and captured using CaseViewer software. The ROIs were then loaded and measured regarding the area percentage of new bone formation and graft materials using ImageJ (National Institutes of Health, Bethesda, MD, USA).

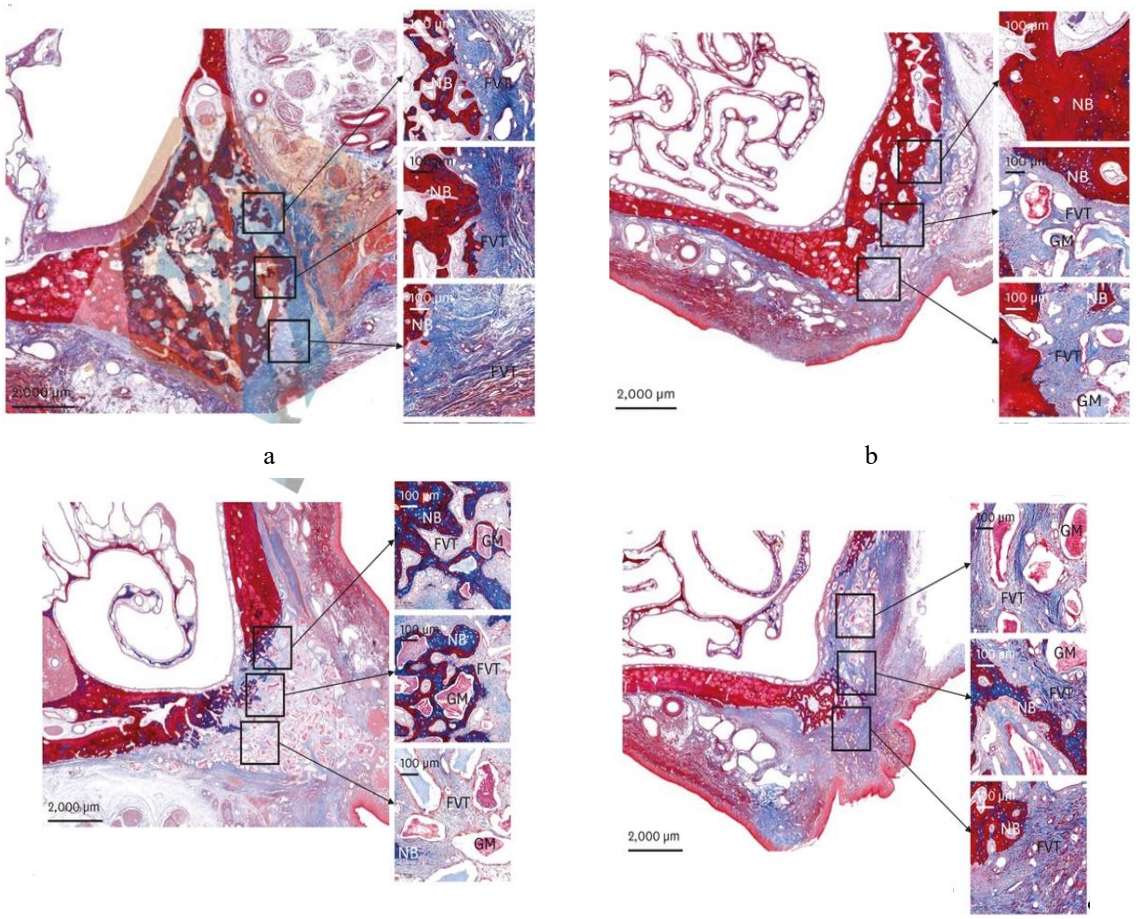

Figure 3. Representative histological view of socket healing at 4 weeks. (a) A spontaneously healed 3-wall defect site is superimposed with the retained contralateral tooth. (b) A 3-wall defect site with alveolar ridge preservation, superimposed with the retained contralateral tooth. (c) A 2-wall defect site with alveolar ridge preservation, superimposed with the retained contralateral tooth. (d) A 1-wall defect site with alveolar ridge preservation, superimposed with the retained contralateral tooth.
NB: new bone, FVT: fibrovascular connective tissue, GM: graft material.

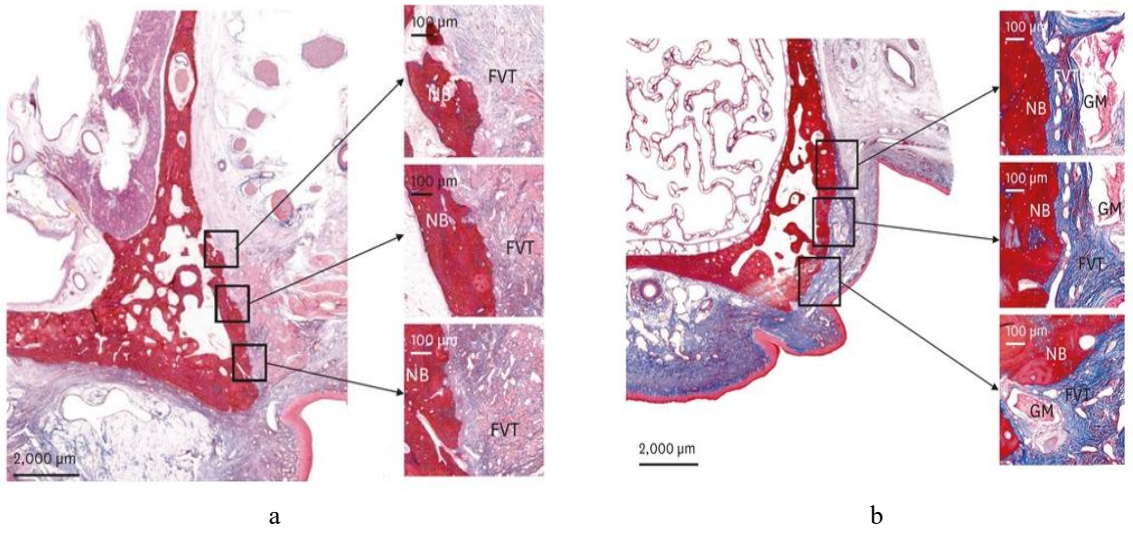

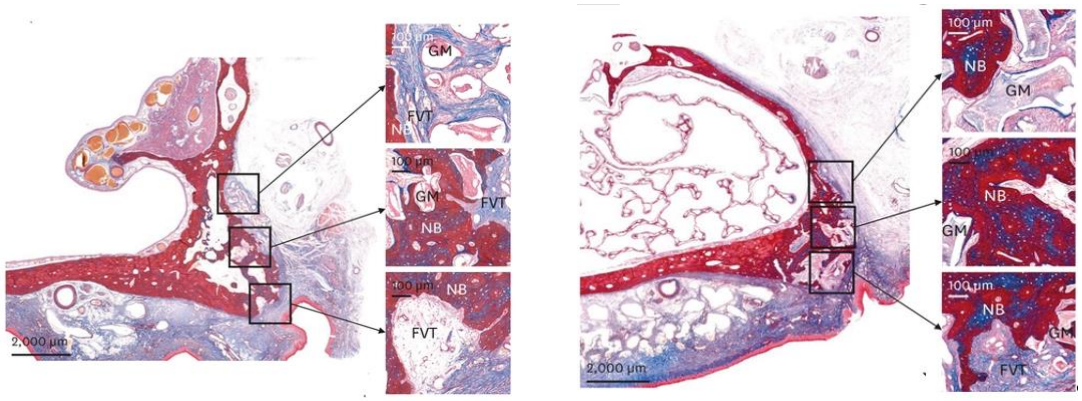

c d

Figure 4. Representative histological view of socket healing at 12 weeks. (a) A spontaneously healed 3-wall defect site is superimposed with the retained contralateral tooth. (b) A 3-wall defect site with alveolar ridge preservation, superimposed with the retained contralateral tooth. (c) A 2-wall defect site with alveolar ridge preservation, superimposed with the retained contralateral tooth. (d) A 1-wall defect site with alveolar ridge preservation, superimposed with the retained contralateral tooth.
NB: new bone, FVT: fibrovascular connective tissue, GM: graft material.

For the quantitative histometric analysis, the contralateral root was vertically superimposed, extending from the crest to 3 mm below it. The following regions were then measured **(Figure 5)**:

- The reference area, on the superimposed image, was the region delineated by the inner surface of the palatal bone and the outermost border of the buccal bone.
- The augmented area, positioned within the reference area, referred to the space demarcated by the clustered graft materials and the newly formed bone.
- The regenerated area, also within reference area, was defined as the region including the newly formed bone.

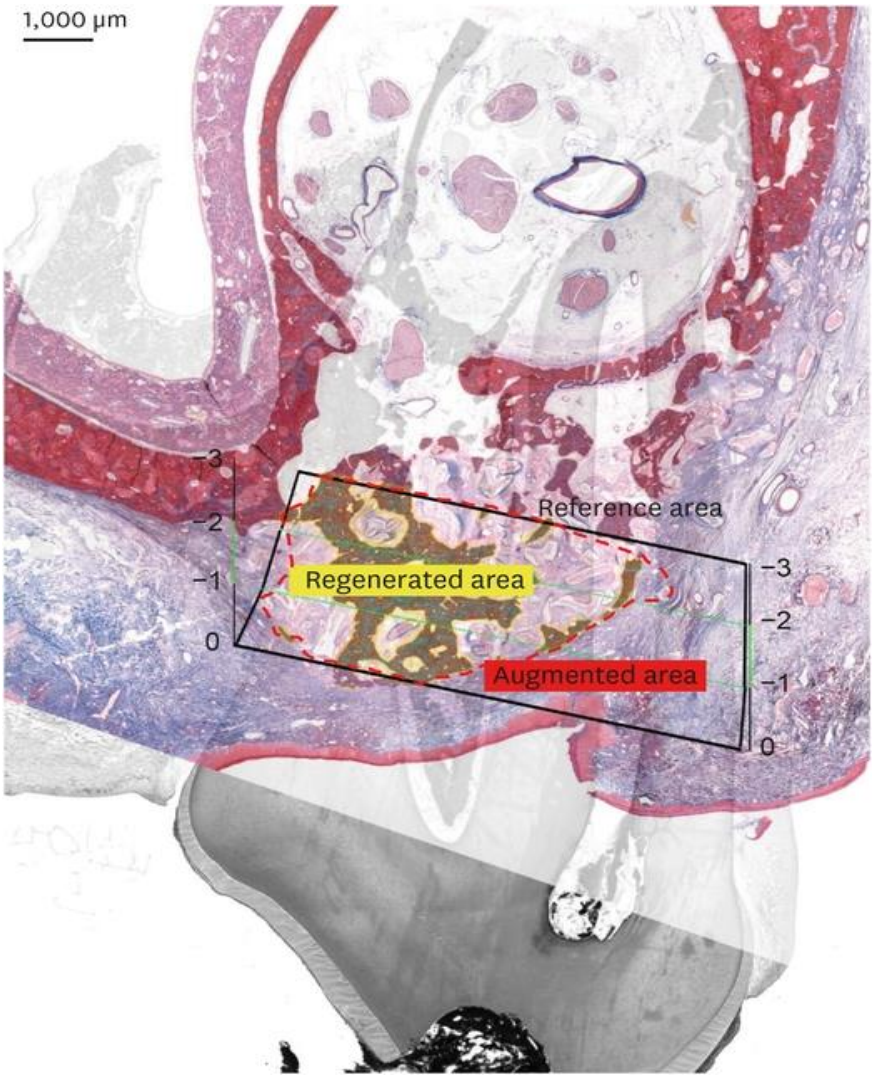

Figure 5. Representative histological image for qualitative analysis. Images from symmetrical sites of the same tooth were superimposed. The reference area was established based on the vertical location of the buccal and palatal bony walls surrounding the opposite root. The regenerated and augmented areas within the reference area are marked with yellow and red dotted lines, respectively.

The augmented and regenerated areas within the reference area were measured using ImageJ. The percentage of mineralization in the augmented area was calculated as follows:

$$-\ Mineralization\ Percentage = \frac{Regenerated\ Area}{Reference\ Area} \times 100 \quad (1)$$

For qualitative and quantitative histometric analyses, a specialist took 3 measurements weekly and averaged the results.

Statistical analysis

Statistical analyses were performed using SPSS (version 25.0, IBM Corp., Armonk, NY, USA). Outcome data are presented as mean ± SD or as median (minimum–maximum) with interquartile range. The Mann-Whitney *U* test and the Kruskal-Wallis test were utilized for histomorphometric analyses. To assess variables potentially related to the percentage of mineralization, the generalized estimating equation (GEE) procedure was employed. A *P* value of less than 0.05 was considered to indicate statistical significance.

Results and Discussion

Clinical findings

Eight beagle dogs were included in the analysis for the 4-week and 12-week healing periods. Uneventful healing, without any signs of inflammation, was observed at all experimental sites. Volumetric shrinkage was more pronounced in the 1-wall defect than in the 2- or 3-wall defects, regardless of the application of ARP.

Histological description

All experimental sites exhibited no signs of inflammation, with integrated graft materials and new bone present in the augmented areas. A time-dependent increase in bone mineralization was observed. In the ARP group, trabecular new bone formation was evident in the augmented area. The trabecular spaces were filled with residual graft materials and connective tissue, including blood vessels. Greater new bone formation was observed with increasing depth from the crestal bone.

Histomorphometric analysis

Qualitative histometric analysis of SH and ARP groups

Qualitative histometric outcomes comparing the 1-wall, 2-wall, and 3-wall defects at both SH and ARP sites are presented in **Table 1**. After a 4-week healing period, no significant differences were observed among the 1-, 2-, and 3-wall defects at either SH or ARP sites. Similarly, after a 12-week healing period, no significant differences were observed among the defects at these sites. At 4 weeks, the percentage of new bone was greater in the apical area compared to the coronal area.

Table 1. Qualitative histometric analysis of SH and ARP groups

Time	Location	Defect	SH			ARP		
			NB	GM	FVT	NB	GM	FVT
4 weeks	Apical	1-wall	61.53±8.41	-	38.48±8.41	48.5±33.90	5.35±10.7	46.15±23.98
			63.15 (51–69), 16		36.35 (31–50), 16	58.60 (0–77), 61	0 (0–21), 16	41.40 (23–79), 45
		2-wall	24.93±25.09	-	75.08±25.09	63.35±15.11	3.25±6.5	33.40±18.02
			20.00 (0–60), 46		80 (40–100), 46	66.15 (43–78), 28	0 (0–13), 10	29.50 (17–57), 34
		3-wall	26.70±23.69	-	73.30±23.69	45.40±21.84	5.1±6.13	49.50±17.49
			25.05 (0–57), 45		74.95 (43–100), 45	46.20 (20–70), 42	4.05 (0–12), 11	47.65 (30–72), 33
		P value	0.087	-	0.087	0.551	0.915	0.472
	Middle	1-wall	40.58±11.03	-	59.43±11.03	25.50±22.92	9.35±9.13	65.15±19.93
			41.75 (26–53), 20		58.25 (47–74), 20	24 (0–54), 44	7.9 (0–22), 17	73.1 (36–78), 34
		2-wall	20.05±21.04	-	79.50±21.04	28.53±41.30	8.40±5.79	63.07±35.55
			16.01 (0–50), 39		83.9 (50–100), 39	12.3 (0–90), 70	10.65 (0–12), 10	77.05 (11–88), 60
		3-wall	28.85±25.17	-	71.15±25.17	31.15±14.26	8.28±5.67	60.58±14.25
			32.6 (0–50), 46		67.4 (50–100), 46	37 (10–41), 24	10.15 (0–13), 10	56.6 (49–80), 26
		P value	0.414	-	0.414	0.683	0.981	0.668
	Coronal	1-wall	16.00±10.27	-	84.00±10.27	4.08±8.15	16.58±8.1	79.35±6.23
			16.25 (5–26), 19		83.75 (74–95), 19	0 (0–16), 12	16.7 (8–25), 15	76.9 (75–89), 11
		2-wall	26.08±23.33	-	73.93±23.33	3.38±6.75	17.7±12.48	78.93±7.92
			27.30 (0–50), 44		72.70 (50–100), 44	0 (0–14), 10	17.85 (2–33), 23	82.15 (67–84), 13
		3-wall	7.95±9.25	-	92.05±9.25	3.95±4.64	14.25±7.81	81.80±6.71
			7.25 (0–17), 17		92.75 (83–100), 17	3.4 (0–9), 8	10.75 (10–26), 13	81.55 (74–90), 13
		P value	0.467	-	0.467	0.915	0.904	0.841

12 weeks	Apical	1-wall	31.45±18.86	-	68.55±18.86	59.38±20.27	9.00±10.65	31.63±24.28
			36.35 (6–48), 35		63.65 (52–95), 35	60.25 (37–81), 39	7.50 (0–21), 19	27.8 (7–64), 46
		2-wall	39.13±14.94	-	60.88±14.94	48.50±24.69	21.0±13.65	30.50±11.72
			34.25 (27–61), 27		65.75 (39–73), 27	43.70 (27–80), 46	22.25 (6–34), 25	33.1 (14–42), 46
		3-wall	51.97±24.81	-	48.03±24.81	75.83±1.80	3.55±4.27	20.63±5.5
			51.65 (30–75), 44		48.35 (25–70), 44	75.35 (74–78), 3	2.80 (0–9), 8	22.35 (13–25), 10
		P value	0.551	-	0.551	0.334	0.128	0.551
	Middle	1-wall	42.55±19.17	-	57.45±19.17	29.05±12.62	16.73±11.53	54.23±21.68
			42.70 (21–63), 37		57.30 (37–79), 37	24.00 (20–48), 21	20.08 (0–25), 20	55.20 (27–80), 41
		2-wall	36.22±19.57	-	63.78±19.57	46.93±17.18	25.20±9.74	27.88±12.52
			34.85 (14–62), 36		65.15 (39–86), 36	47.15 (31–63), 31	28.01 (11–34), 17	31.00 (11–39), 28
		3-wall	39.63±16.84	-	39.38±26.92	51.58±33.06	27.73±26.17	20.7±7.58
			43.30 (16–56), 30		49.95 (0–58), 46	52.00 (12–90), 64	24.95 (0–61), 50	23.05 (10–27), 14
		P value	0.874	-	0.368	0.309	0.537	0.037[b)]
	Coronal	1-wall	49.75±6.29	-	50.25±6.29	12.38±8.40	9.78±19.55	77.85±18.20
			47.50 (45–59), 11		52.50 (41–55), 11	9.00 (7–25), 14	0 (0–39), 29	82.45 (53–93), 34
		2-wall	37.53±29.30	-	54.18±42.22	37.98±22.54	26.65±20.44	35.38±5.64
			39.90 (4–67), 56		60.10 (0–97), 81	44.25 (6–58), 40	24.00 (5–54), 38	36.95 (27–40), 10
		3-wall	39.75±35.01	-	35.25±32.79	25.48±20.40	31.25±20.39	43.27±28.00
			36.85 (0–85), 65		38.10 (0–65), 60	27.10 (0–48), 39	30.10 (9–56), 39	42.30 (10–79), 52
		P value	0.668	-	0.828	0.390	0.227	0.037[a)]

Values are presented as mean ± standard deviation or median (minimum–maximum), interquartile range.
SH: spontaneous healing, ARP: alveolar ridge preservation, NB: new bone, GM: graft material, FVT: fibrovascular connective tissue.
[a)]*P*<0.05 between 1-wall and 2-wall groups; [b)]*P*<0.05 between 1-wall and 3-wall groups.

Quantitative histometric analysis of SH and ARP groups

Quantitative histometric analysis was used to compare 1-wall, 2-wall, and 3-wall defects at both SH and ARP sites, as shown in **Table 2**. Twelve specimens from each healing group (4 weeks and 12 weeks) were allocated and analyzed. The percentage of mineralization between SH and ARP at each defect site was not statistically significant at 4 weeks. Additionally, the percentage of mineralization according to defect type did not differ significantly in either the SH or the ARP group at 4 weeks.

Table 2. Quantitative histometric analysis of SH and ARP groups

Time	Variables	Defect	SH	ARP	*P* value
4 weeks	Reference area (mm^2)	1-wall	11.73±4.12	10.30±2.98	1
			11.45 (7.87–16.15), 7.64	9.16 (8.16–14.7), 5.07	
		2-wall	9.42±2.29	12.36±8.76	0.886
			8.95 (7.19–12.58), 4.26	8.46 (7.1–25.4), 14.12	
		3-wall	12.13±8.07	13.86±9.05	1
			8.42 (7.45–24.22), 12.77	10.22 (7.85–27.16), 15.37	
		P value	0.779	0.694	
	Augmented area (mm^2)	1-wall	-	7.41±1.10	-
				7.34 (6.13–8.83), 2.05	
		2-wall	-	7.15±3.34	-
				6.19 (4.41–11.82), 6.11	
		3-wall	-	11.62±9.75	-
				7.81 (4.99–25.88), 16.75	
		P value	-	0.794	

	Regenerated area (mm^2)	1-wall	3.94±1.43	4.18±1.56	1
			4.39 (1.89–5.09), 2.55	3.97 (2.54–6.25), 2.97	
		2-wall	5.04±2.90	4.08±4.58	0.886
			4.16 (2.6–9.26), 5.03	3.1 (0–10.14), 8.59	
		3-wall	3.97±2.22	4.84±4.62	1
			3.95 (1.28–6.69), 4.19	2.99 (1.73–11.66), 7.78	
		P value	0.874	0.841	
	Augmented/reference area (%)	1-wall	-	76.00±22.67	-
				76.84 (50–100), 43	
		2-wall	-	63.43±13.55	-
				63.92 (46–79), 26	
		3-wall	-	77.22±14.72	-
				75.02 (64–95), 28	
		P value	-	0.39	
	Mineralization percentage (%)	1-wall	35.27±14.39	42.50±19.33	0.486
			30.5 (24.0–55.0), 26	34.5 (30–71), 32	
		2-wall	52.25±19.00	47.25±27.14	0.343
			53.5 (28.0–74.0), 36	53 (12–71), 51	
		3-wall	35.50±16.36	32.5±13.77	0.686
			38.0 (16.0–50.0), 31	36.5 (14–43), 51	
		P value	0.234	0.788	
12 weeks	Reference area (mm^2)	1-wall	12.01±2.93	16.01±8.13	0.686
			12.73 (7.93–14.67), 5.41	15.98 (8.82–23.28), 14.28	
		2-wall	9.35±2.04	11.53±6.02	1
			8.91 (7.55–12.02), 3.83	8.91 (7.77–20.53), 9.65	
		3-wall	12.28±7.72	10.04±2.54	1
			10.14 (5.77–23.11), 14.15	9.17 (8.12–13.74), 4.47	
		P value	0.437	0.309	
	Augmented area (mm^2)	1-wall	-	10.49±2.62	-
				10.62 (7.2–13.55), 5.01	
		2-wall	-	7.65±2.69	-
				6.51 (5.93–11.67), 4.43	
		3-wall	-	8.15±1.36	-
				7.78 (7.01–10.05), 2.5	
		P value	N/A	0.174	
	Regenerated area (mm^2)	1-wall	3.65±0.63	6.81±3.32	0.200
			3.72 (2.82–4.34), 1.18	7.04 (3.2–9.98), 6.2	
		2-wall	3.94±0.82	5.35±1.19	0.114
			3.77 (3.22–5.01), 1.55	5.14 (4.12–6.99), 2.18	
		3-wall	5.83±3.38	6.09±0.96	0.486
			4.85 (3.01–10.63), 6.16	6.14 (4.87–7.23), 1.78	
		P value	0.551	0.779	
	Augmented/reference area (%)	1-wall	-	72.18±23.27	-
				70.48 (48–100), 45	
		2-wall	-	69.91±10.16	-
				71.17 (57–80), 19	
		3-wall	-	82.48±12.12	-
				78.39 (73–100), 21	
		P value	-	0.469	
	Mineralization percentage (%)	1-wall	34.06±15.07	43.15±7.08	0.343
			31.16 (19.0–55.0), 28	41.75 (36.0–53.0), 13	
		2-wall	42.89±8.98	50.65±11.29	0.343

		41.08 (34.0–55.0), 16	55.24 (34.0–58.0), 19	
3-wall		48.84±3.05	61.73±7.5	0.029[a)]
		48.59 (46.0–52.0), 6	61.8 (53.0–71.0), 14	
P value		0.292	0.077	

Values are presented as mean ± standard deviation or median (minimum–maximum), interquartile range.
SH, spontaneous healing; ARP, alveolar ridge preservation, N/A: not available.
Mineralization Percentage =
[a)]*P*<0.05.

For 1-wall and 2-wall defects, the percentage of mineralization was not significantly different between SH and ARP at 12 weeks. In contrast, for 3-wall defects, the SH and ARP groups did significantly differ in the percentage of mineralization at 12 weeks, with values of 48.84%±3.06% in the SH group versus 61.73%±7.52% in the ARP group (*P*=0.029). In intragroup analysis, the percentage of mineralization increased with the number of bony walls; however, no statistical differences were observed. GEE analysis indicated that both defect type and healing time significantly influenced the percentage of mineralization. Additionally, interaction effects were exhibited by defect type, intervention, and healing time, as shown in **Table 3**.

Table 3. Predictors of mineralization percentage

Variables	Wald	*P* value
Defect type (1-, 2-, or 3-wall)	14.30	<0.001
Healing time (4 or 12 wk)	5.40	0.02
Intervention (SH or ARP)	0.12	0.72
Defect type × intervention	9.32	0.01
Defect type × healing time	40.85	<0.001
Healing time × intervention	5.20	0.02
Defect type × healing time × intervention	57.95	<0.001

Generalized estimation equation analysis was applied.
SH: spontaneous healing, ARP: alveolar ridge preservation.

The aim of this study was to evaluate the bone healing potential of 1-, 2-, and 3-wall defects during ARP following tooth extraction, using histomorphometric analyses. After 12 weeks of healing, the ARP group exhibited a greater regenerated area and higher percentage of mineralization compared to the SH group. In the 3-wall defect model, the ARP group demonstrated a significantly higher percentage of mineralization compared to the SH group at the same time point. Although not statistically significant, the percentage of mineralization at 12 weeks for both groups increased in conjunction with the number of bony walls present.

Previous studies have focused on volumetric changes, demonstrating that ARP can reduce both horizontal and vertical bone resorption relative to SH after tooth extraction [25, 26]. A recent clinical study investigating the effectiveness of ARP in periodontally compromised extraction sockets found that ARP was effective in reducing the extent of ridge resorption [15]. However, the impact of the number of remaining bony walls on ARP outcomes has not been thoroughly explored. In the present study, in both SH and ARP groups, we observed a higher percentage of mineralization as the number of bony walls increased, although this finding did not reach statistical significance. Notably, the mineralization percentage in the ARP group was significantly higher than in the SH group for 3-wall defects (*P*=0.029). These findings suggest that the number of bony walls may influence bone healing in the extracted socket, as the bony wall serves as a source of regeneration for ARP.

Healing time is known to contribute to the increase in new bone formation when ARP is applied. A clinical study showed that a group with a longer duration of healing demonstrated significantly more new bone than a group with a shorter healing time [27]. Similarly, a greater amount of mineralized tissue was observed in the group with extended healing compared to the control group [28]. Our study confirmed a similar trend. The group with a 12-week healing period exhibited a higher rate of regeneration compared to the 4-week healing group. A clearly higher percentage of mineralization was observed in the 12-week healing group, regardless of the number of remaining bony walls. The optimal time for osteogenesis, which may be influenced by the amount of remaining bone, appears to be more likely to be 12 weeks than 4 weeks.

The provisional matrix, along with blood vessels and pleiotropic macrophages from adjacent pristine bone, facilitates new bone formation [29]. Previous research has shown that a greater number of pristine bone walls

provides a more favorable environment regarding healing potential following guided bone regeneration [30]. In this context, it is anticipated that the regeneration rate would be higher in ARP in a 3-wall defect compared to a 1-wall defect. In our study, the percentage of mineralization tended to increase with the number of remaining bony walls. Notably, however, these results lacked statistical significance. Previous studies have demonstrated that porcine bone induces comparable bone formation and volume stability to that of bovine bone [31, 32]. However, the resorption characteristics of porcine bone have been reported to show no signs of osteoclastic activity and to exhibit continuous resorption at certain times [33, 34]. The inconsistent resorption rates of porcine bone might have affected those results. Thus, future studies should investigate the resorption pattern of the porcine bone used.
In our study, flap reflection was performed during the ARP procedure, and the flap was secured with sutures following ARP due to the acute defect model used. The question arises as to whether the stability of soft tissue achieved through primary wound closure creates a conducive environment for new bone formation. Primary closure following ARP might diminish the influence of the defect walls on the percentage of mineralization. Although a recent study of periodontally compromised extraction sockets demonstrated that ARP without primary closure resulted in comparable new bone formation and radiographic ridge volume to ARP with primary closure [35], the importance of wound stability in bone regeneration should still be considered.
Our study had several limitations. First, the small sample size within each subgroup (that is, the number of defect walls and interventions) could have influenced the results. Although defect type was identified as a predictor for the percentage of mineralization, statistical significance was not achieved. Second, the ridge shape on the contralateral side may have differed from that on the original side in the beagle dogs. Variations in the precise location and 3-dimensional (3D) alignment of the histological sections make accurate comparisons challenging. Third, anatomical structures such as the palatal bone and irregular sinuses can affect the outcome of ARP. Since dogs lack a palatal vault, complete removal of the palatal wall is sometimes difficult. In this context, using lower teeth rather than upper teeth might be preferable to minimize variables that influence bone healing. Fourth, 3D evaluation using micro-computed tomography (micro-CT) was not performed, most notably for quantitative measurements. Future studies should employ micro-CT to facilitate 3D evaluations.
Within the limitations of this study, ARP treatment for compromised sockets tends to result in a higher percentage of mineralization compared to SH. The type of defect, healing time, and intervention appear to influence the percentage of mineralization. Although the effectiveness of the remaining bony walls was limited, their presence appeared to improve the percentage of mineralization in ARP treatment.

Acknowledgments: None

Conflict of interest: None

Financial support: This work was supported by a grant from the Seoul National University Dental Hospital Research Fund (No. 08-2023-0022). We would like to express our gratitude to Professor Youngha Song for reviewing the statistical analysis.

Ethics statement: None

References

1. Tan WL, Wong TLT, Wong MCM, Lang NP. A systematic review of post-extractional alveolar hard and soft tissue dimensional changes in humans. Clin Oral Implants Res. 2012;23(Suppl 5):1–21.
2. Aimetti M, Romano F, Griga FB, Godio L. Clinical and histologic healing of human extraction sockets filled with calcium sulfate. Int J Oral Maxillofac Implants. 2009;24(5):902–9.
3. Barone A, Aldini NN, Fini M, Giardino R, Calvo Guirado JL, Covani U. Xenograft versus extraction alone for ridge preservation after tooth removal: a clinical and histomorphometric study. J Periodontol. 2008;79(8):1370–7.
4. Darby I, Chen ST, Buser D. Ridge preservation techniques for implant therapy. Int J Oral Maxillofac Implants. 2009;24(Suppl):260–71.

5. Bienz SP, Ruales-Carrera E, Lee WZ, Hämmerle CHF, Jung RE, Thoma DS. Early implant placement in sites with ridge preservation or spontaneous healing: histologic, profilometric, and CBCT analyses of an exploratory RCT. J Periodontal Implant Sci. 2024;54(2):108–21.
6. Pickert FN, Spalthoff S, Gellrich NC, Blaya Tárraga JA. Cone-beam computed tomographic evaluation of dimensional hard tissue changes following alveolar ridge preservation techniques of different bone substitutes: a systematic review and meta-analysis. J Periodontal Implant Sci. 2022;52(1):3–27.
7. Kim JH, Susin C, Min JH, Suh HY, Sang EJ, Ku Y, et al. Extraction sockets: erratic healing impeding factors. J Clin Periodontol. 2014;41(1):80–5.
8. Kim JH, Koo KT, Capetillo J, Kim JJ, Yoo JM, Ben Amara H, et al. Periodontal and endodontic pathology delays extraction socket healing in a canine model. J Periodontal Implant Sci. 2017;47(3):143–53.
9. Kim JJ, Ben Amara H, Chung I, Koo KT. Compromised extraction sockets: a new classification and prevalence involving both soft and hard tissue loss. J Periodontal Implant Sci. 2021;51(2):100–13.
10. Kim JJ, Schwarz F, Song HY, Choi Y, Kang KR, Koo KT. Ridge preservation of extraction sockets with chronic pathology using Bio-Oss® Collagen with or without collagen membrane: an experimental study in dogs. Clin Oral Implants Res. 2017;28(6):727–33.
11. Kim JJ, Ben Amara H, Park JC, Kim S, Kim TI, Seol YJ, et al. Biomodification of compromised extraction sockets using hyaluronic acid and rhBMP-2: an experimental study in dogs. J Periodontol. 2019;90(4):416–24.
12. Lee J, Lee YM, Lim YJ, Kim B. Ridge augmentation using β-tricalcium phosphate and biphasic calcium phosphate sphere with collagen membrane in chronic pathologic extraction sockets with dehiscence defect: a pilot study in beagle dogs. Materials (Basel). 2020;13:1452.
13. Ben Amara H, Kim JJ, Kim HY, Lee J, Song HY, Koo KT, et al. Is ridge preservation effective in the extraction sockets of periodontally compromised teeth? A randomized controlled trial. J Clin Periodontol. 2021;48(4):464–77.
14. Kim JJ, Ben Amara H, Schwarz F, Kim HY, Lee JW, Wikesjö UM, et al. Is ridge preservation/augmentation at periodontally compromised extraction sockets safe? A retrospective study. J Clin Periodontol. 2017;44(10):1051–8.
15. Lee J, Yun J, Kim JJ, Koo KT, Seol YJ, Lee YM. Retrospective study of alveolar ridge preservation compared with no alveolar ridge preservation in periodontally compromised extraction sockets. Int J Implant Dent. 2021;7:23.
16. Koo TH, Song YW, Cha JK, Jung UW, Kim CS, Lee JS. Histologic analysis following grafting of damaged extraction sockets using deproteinized bovine or porcine bone mineral: a randomized clinical trial. Clin Oral Implants Res. 2020;31(1):93–102.
17. Lee JS, Cha JK, Kim CS. Alveolar ridge regeneration of damaged extraction sockets using deproteinized porcine versus bovine bone minerals: a randomized clinical trial. Clin Implant Dent Relat Res. 2018;20(5):729–37.
18. Nibali L, Sultan D, Arena C, Pelekos G, Lin GH, Tonetti M, et al. Periodontal infrabony defects: systematic review of healing by defect morphology following regenerative surgery. J Clin Periodontol. 2021;48(1):100–13.
19. Chappuis V, Araújo MG, Buser D. Clinical relevance of dimensional bone and soft tissue alterations post-extraction in esthetic sites. Periodontol 2000. 2017;73:73–83.
20. Schwarz F, Sahm N, Schwarz K, Becker J. Impact of defect configuration on the clinical outcome following surgical regenerative therapy of peri-implantitis. J Clin Periodontol. 2010;37(5):449–55.
21. Kim YT, Jeong SN, Lee JH. Effectiveness of porcine-derived xenograft with enamel matrix derivative for periodontal regenerative treatment of intrabony defects associated with a fixed dental prosthesis: a 2-year follow-up retrospective study. J Periodontal Implant Sci. 2021;51(3):179–88.
22. Lee JS, Choe SH, Cha JK, Seo GY, Kim CS. Radiographic and histologic observations of sequential healing processes following ridge augmentation after tooth extraction in buccal-bone-deficient extraction sockets in beagle dogs. J Clin Periodontol. 2018;45(11):1388–97.
23. Bunyaratavej P, Wang HL. Collagen membranes: a review. J Periodontol. 2001;72(2):215–29.
24. Percie du Sert N, Ahluwalia A, Alam S, Avey MT, Baker M, Browne WJ, et al. Reporting animal research: Explanation and elaboration for the ARRIVE guidelines 2.0. PLoS Biol. 2020;18(7):e3000411.

25. Avila-Ortiz G, Chambrone L, Vignoletti F. Effect of alveolar ridge preservation interventions following tooth extraction: a systematic review and meta-analysis. J Clin Periodontol. 2019;46(Suppl 21):195–223.
26. Lim HC, Shin HS, Cho IW, Koo KT, Park JC. Ridge preservation in molar extraction sites with an open-healing approach: a randomized controlled clinical trial. J Clin Periodontol. 2019;46(10):1144–54.
27. Zellner JW, Allen HT, Kotsakis GA, Mealey BL. Wound healing after ridge preservation: a randomized controlled trial on short-term (4 months) versus long-term (12 months) histologic outcomes. J Periodontol. 2023;94(4):622–29.
28. Couso-Queiruga E, Weber HA, Garaicoa-Pazmino C, Barwacz C, Kalleme M, Galindo-Moreno P, et al. Influence of healing time on the outcomes of alveolar ridge preservation using a collagenated bovine bone xenograft: a randomized clinical trial. J Clin Periodontol. 2023;50(1):132–46.
29. Gruber R, Stadlinger B, Terheyden H. Cell-to-cell communication in guided bone regeneration: molecular and cellular mechanisms. Clin Oral Implants Res. 2017;28(10):1139–46.
30. Benic GI, Hämmerle CH. Horizontal bone augmentation by means of guided bone regeneration. Periodontol 2000. 2014;66(1):13–40.
31. Lee JS, Shin HK, Yun JH, Cho KS. Randomized clinical trial of maxillary sinus grafting using deproteinized porcine and bovine bone mineral. Clin Implant Dent Relat Res. 2017;19(1):140–50.
32. Krennmair S, Postl L, Schwarze UY, Malek M, Stimmelmayr M, Krennmair G. Clinical, radiographic, and histological/histomorphometric analysis of maxillary sinus grafting with deproteinized porcine or bovine bone mineral: a randomized clinical trial. Clin Oral Implants Res. 2023;34(9):1230–47.
33. Nannmark U, Sennerby L. The bone tissue responses to prehydrated and collagenated cortico-cancellous porcine bone grafts: a study in rabbit maxillary defects. Clin Implant Dent Relat Res. 2008;10(4):264–70.
34. Orsini G, Scarano A, Piattelli M, Piccirilli M, Caputi S, Piattelli A. Histologic and ultrastructural analysis of regenerated bone in maxillary sinus augmentation using a porcine bone-derived biomaterial. J Periodontol. 2006;77(11):1984–90.
35. Seo GJ, Lim HC, Chang DW, Hong JY, Shin SI, Kim G, et al. Primary flap closure in alveolar ridge preservation for periodontally damaged extraction socket: a randomized clinical trial. Clin Implant Dent Relat Res. 2023;25(2):241–51.